arXiv:hep-ph/0101110v2 9 Mar 2001

Current quark mass effects on chiral phase transition of QCD in the improved ladder approximation

O. Kiriyama *
Research Center for Nuclear Physics, Osaka University, Ibaraki 567–0047, Japan

M. Maruyama † and F. Takagi‡
Department of Physics, Tohoku University, Sendai 980–8578, Japan

Current quark mass effects on the chiral phase transition of QCD is studied in the improved ladder approximation. An infrared behavior of the gluon propagator is modified in terms of an effective running coupling. The analysis is based on a composite operator formalism and a variational approach. We use the Schwinger-Dyson equation to give a "normalization condition" for the Cornwall-Jackiw-Tomboulis effective potential and to isolate the ultraviolet divergence which appears in an expression for the quark-antiquark condensate. We study the current quark mass effects on the order parameter at zero temperature and density. We then calculate the effective potential at finite temperature and density and investigate the current quark mass effects on the chiral phase transition. We find a smooth crossover for $T > 0$, $\mu = 0$ and a first-order phase transition for $\mu > 0$, $T = 0$. Critical exponents are also studied and our model gives the classical mean-field values. We also study the temperature dependence of masses of scalar and pseudoscalar bosons. A critical end point in the T-μ plane is found at $T \sim 100$ MeV, $\mu \sim 300$ MeV.

PACS number(s): 11.10.Wx, 11.15.Tk, 11.30.Rd, 12.38.Lg

I. INTRODUCTION

Recently there has been great interest in studying the phase structure of quantum chromodynamics (QCD). We expect that at sufficiently high temperature and/or density the QCD vacuum changes into a chirally symmetric/ deconfinement phase [1], a color superconducting phase [2–4] or a color-flavor locked phase [5]. They may be realized in high-energy heavy-ion collisions at the BNL Relativistic Heavy Ion Collider and CERN Large Hadron Collider. These phase transitions are important also in the physics of neutron stars and the early universe.

The phase structure of QCD has been studied by various methods. At finite temperature the lattice simulation is powerful for studying the phase structure of QCD. On the other hand, the so-called QCD-like theories, one category of the effective theories of QCD, are still useful for studying the chiral phase structure at high temperature and/or density [6–15]. QCD in the weak coupling limit is utilized to study the color superconductivity [2–5]. However, most studies have been done in the zero external field limit; i.e., in the chiral limit for the case of the dynamical chiral symmetry breaking. It is, then, desirable to study a more realistic situation where the chiral symmetry is explicitly broken by a current quark mass. In this paper we neglect the quark pairing and study the current quark mass effects on the chiral phase transition between $SU(N_c) \times SU(N_f)_L \times SU(N_f)_R$ and $SU(N_c) \times SU(N_f)_{L+R}$. In order to study nonperturbative phenomena such as the dynamical chiral symmetry breaking, the Schwinger-Dyson equation (SDE) or the effective potential for a composite operator has been widely used. However, in order to find the true vacuum it is necessary to calculate the effective potential. Furthermore, in the studies of the SDE, it was known that there is a difficulty in removing a perturbative contribution which is quadratically divergent from the order parameter of chiral symmetry [16,17].

Our analysis starts from the Cornwall-Jackiw-Tomboulis (CJT) effective action for a composite operator [18] and QCD in the improved ladder (rainbow) approximation [19–21]. The improved ladder approximation is the simplest nonperturbative truncation scheme which is consistent with the renormalization group. At zero temperature and density, it reproduces the physical quantities which are insensitive to the model parameter [22]. Therefore, we expect that it is valid also at finite temperature and/or density. We use the SDE to modify the CJT effective potential. The result is used to give a "normalization condition" for the effective potential [23] and to isolate the ultraviolet

*Email address: kiriyama@rcnp.osaka-u.ac.jp
†Email address: maruyama@nucl.phys.tohoku.ac.jp
‡Email address: takagi@nucl.phys.tohoku.ac.jp

divergence which appears in an expression for quark-antiquark condensate. The divergence depends solely on the qurak mass and is independent of the condensate.

This paper is organized as follows. In Sec. II we derive the modified form of the CJT effective potential for quark propagator at zero temperature and density. The critical value of the coupling constant and the critical number of quark flavors are examined for comparison with the results by other authors. We then extend the modified effective potential to finite temperature and density. In Sec. III we first determine the value of $\Lambda_{\rm QCD}$ by a condition $f_\pi = 93$ MeV at $T = \mu = 0$ and in the chiral limit. Then we calculate the effective potential numerically and investigate the phase structure for nonzero T, μ and nonzero current quark mass. We also examine the critical exponents, the temperature dependence of masses of the scalar and pseudoscalar bosons and the critical end point. Section IV is devoted to the summary and discussion. We fix the mass scale by the condition $\Lambda_{\rm QCD} = 1$ except for numerical calculations.

II. EFFECTIVE POTENTIAL FOR THE QUARK PROPAGATOR

A. CJT effective potential at zero temperature and density

At zero temperature and zero density, the CJT effective potential for QCD in the improved ladder approximation is expressed as a functional of $S(p)$ the quark full propagator [19]:

$$V[S] = V_1[S] + V_2[S], \tag{1}$$

$$V_1[S] = \int \frac{d^4p}{(2\pi)^4 i}\ {\rm Tr}\left\{\ln[S_0^{-1}(p)S(p)] - S_0^{-1}(p)S(p) + 1\right\}, \tag{2}$$

$$V_2[S] = -\frac{i}{2}C_2 \int\int \frac{d^4p}{(2\pi)^4 i}\ \frac{d^4q}{(2\pi)^4 i}\ \bar{g}^2(p,q){\rm Tr}\left[\gamma_\mu S(p)\gamma_\nu S(q)\right] D^{\mu\nu}(p-q), \tag{3}$$

where $C_2 = (N_c^2 - 1)/(2N_c)$ is the quadratic Casimir operator for the color $SU(N_c)$ group, $S_0(p)$ is the bare quark propagator, $\bar{g}^2(p,q)$ is the QCD running coupling of one-loop order, $D^{\mu\nu}(p)$ is the gluon propagator which is diagonal in the color space and, "Tr" refers to Dirac, flavor, and color matrices. The two-loop potential V_2 is given by the vacuum graph of the fermion one-loop diagram with one-gluon exchange.

After Wick rotation, we use the following approximation

$$\bar{g}^2(p_E, q_E) = \theta(p_E - q_E)\bar{g}^2(p_E) + \theta(q_E - p_E)\bar{g}^2(q_E). \tag{4}$$

This approximation is occasionally called Higashijima-Miransky approximation [19,20]. In this approximation and in the Landau gauge, renormalization of the quark wave function is unnecessary and the CJT effective potential is expressed in terms of $\Sigma(p_E)$, the dynamical mass function of a quark as follows

$$V[\Sigma(p_E)] = V_1[\Sigma(p_E)] + V_2[\Sigma(p_E)], \tag{5}$$

$$\begin{aligned} V_1[\Sigma(p_E)] = &-2\int^\Lambda \frac{d^4p_E}{(2\pi)^4}\ \ln\frac{\Sigma^2(p_E) + p_E^2}{m^2(\Lambda) + p_E^2} \\ &+4\int^\Lambda \frac{d^4p_E}{(2\pi)^4}\ \frac{\Sigma(p_E)[\Sigma(p_E) - m(\Lambda)]}{\Sigma^2(p_E) + p_E^2}, \end{aligned} \tag{6}$$

$$\begin{aligned} V_2[\Sigma(p_E)] = &-6C_2\int^\Lambda\int^\Lambda \frac{d^4p_E}{(2\pi)^4}\frac{d^4q_E}{(2\pi)^4}\ \frac{\bar{g}^2(p_E,q_E)}{(p_E-q_E)^2} \\ &\times\frac{\Sigma(p_E)}{\Sigma^2(p_E)+p_E^2}\frac{\Sigma(q_E)}{\Sigma^2(q_E)+q_E^2}, \end{aligned} \tag{7}$$

where an overall factor (the number of light quarks times the number of colors) is omitted and $m(\Lambda)$ is the bare quark mass. In the above equations we temporarily introduced the ultraviolet cutoff Λ in order to make the bare quark mass well defined.

The extremum condition for V with respect to the variation of $\Sigma(p_E)$ leads to the following SDE for the quark self-energy

$$\Sigma(p_E) = m(\Lambda) + 3C_2\int^\Lambda \frac{d^4q_E}{(2\pi)^4}\ \frac{\bar{g}^2(p_E,q_E)}{(p_E-q_E)^2}\ \frac{\Sigma(q_E)}{\Sigma^2(q_E)+q_E^2}. \tag{8}$$

In the Higashijima-Miransky approximation, since the argument of the running coupling has no angle dependence, we first perform the angle integration using the result:

$$\int \frac{d\Omega_4}{(p_E - q_E)^2} = \theta(p_E - q_E)\frac{1}{p_E^2} + \theta(q_E - p_E)\frac{1}{q_E^2}, \tag{9}$$

where

$$\int d\Omega_4 = \frac{1}{2\pi^2}\int_0^\pi d\psi \sin^2\psi \int_0^\pi d\theta \sin\theta \int_0^{2\pi} d\phi. \tag{10}$$

Then Eq. (8) is reduced to the following differential equation [16,21]:

$$\frac{\Sigma(p_E)}{\Sigma^2(p_E) + p_E^2} = \frac{(4\pi)^2}{3C_2}\frac{d}{p_E^2 dp_E^2}\left(\frac{1}{\Delta(p_E)}\frac{d\Sigma(p_E)}{dp_E^2}\right), \tag{11}$$

with the two boundary conditions

$$\frac{1}{\Delta(p_E)}\frac{d\Sigma(p_E)}{dp_E^2}\bigg|_{p_E=0} = 0, \tag{12}$$

$$\Sigma(p_E) - \frac{\mathcal{D}(p_E)}{\Delta(p_E)}\frac{d\Sigma(p_E)}{dp_E^2}\bigg|_{p_E=\Lambda} = m(\Lambda), \tag{13}$$

where the functions

$$\mathcal{D}(p_E) = \frac{\bar{g}^2(p_E)}{p_E^2}, \tag{14}$$

and

$$\Delta(p_E) = \frac{d}{dp_E^2}\mathcal{D}(p_E), \tag{15}$$

are introduced.

Substituting Eqs. (8) and (11) into Eqs. (6) and (7), we obtain

$$\begin{aligned}
V[\Sigma(p_E)] &= -2\int^\Lambda \frac{d^4p_E}{(2\pi)^4}\ \ln\frac{\Sigma^2(p_E)+p_E^2}{m^2(\Lambda)+p_E^2} \\
&\quad +2\int^\Lambda \frac{d^4p_E}{(2\pi)^4}\ \frac{\Sigma(p_E)[\Sigma(p_E)-m(\Lambda)]}{\Sigma^2(p_E)+p_E^2} \\
&= -2\int^\Lambda \frac{d^4p_E}{(2\pi)^4}\ \ln\frac{\Sigma^2(p_E)+p_E^2}{m^2(\Lambda)+p_E^2} \\
&\quad +\frac{2(4\pi)^2}{3C_2}\int^\Lambda \frac{d^4p_E}{(2\pi)^4}\ [\Sigma(p_E)-m(\Lambda)]\frac{d}{p_E^2dp_E^2}\left(\frac{1}{\Delta(p_E)}\frac{d\Sigma(p_E)}{dp_E^2}\right) \\
&= -2\int^\Lambda \frac{d^4p_E}{(2\pi)^4}\ \ln\frac{\Sigma^2(p_E)+p_E^2}{m^2(\Lambda)+p_E^2} \\
&\quad -\frac{2}{3C_2}\int^{\Lambda^2} dp_E^2\ \frac{1}{\Delta(p_E)}\left(\frac{d}{dp_E^2}\Sigma(p_E)\right)^2 + V_S,
\end{aligned} \tag{16}$$

where we used a partial integration in the last line and

$$V_S = F(\Lambda) - F(0), \tag{17}$$

$$F(p_E) = \frac{2}{3C_2}\left[\Sigma(p_E) - m(\Lambda)\right]\frac{1}{\Delta(p_E)}\frac{d\Sigma(p_E)}{dp_E^2}. \tag{18}$$

Hereafter, we consider the effective potential in the continuum limit ($\Lambda \to \infty$). Let us begin by evaluating $F(\Lambda)$ using the running coupling

$$\bar{g}^2(p_E) = \frac{2\pi^2 a}{\ln p_E^2} \quad , \quad a \equiv \frac{24}{11N_c - 2n_f}, \tag{19}$$

and the corresponding asymptotic form of the mass function

$$\Sigma(p_E) \to m(\Lambda) \left(\frac{\ln p_E^2}{\ln \Lambda^2} \right)^{-a/2} + \frac{\sigma}{p_E^2} (\ln p_E^2)^{a/2-1}, \tag{20}$$

where n_f is the number of quark flavors which contributes to the running coupling. Throughout this paper, with the exception of discussion on a critical number of massless flavors, we put $N_c = n_f = 3$, namely, $a = 8/9$. As we will show below, the parameter σ is related to the order parameter of chiral symmetry, a.k.a. the quark condensate. Note that Eq. (20) is to be understood in the sense that for exact chiral symmetry the first term on the RHS is zero and the second term is the dominant one, while in the presence of explicit chiral symmetry breaking the first term gives the dominant asymptotic behavior. With the explicit chiral symmetry breaking, there will be many terms which are suppressed by powers of $\ln(p_E^2)$ compared to the first term, but dominate the second term as $p_E^2 \to \infty$ [16].

Using Eqs. (19) and (20), we obtain

$$\begin{aligned} F(\Lambda) &= \frac{2}{3C_2} \cdot \frac{\sigma^2}{\Lambda^2} \, (\ln \Lambda^2)^{a/2-1} \, \frac{\Lambda^4 (\ln \Lambda^2)^2}{\ln \Lambda^2 + 1} \cdot \frac{-1}{2\pi^2 a} \\ &\quad \times \left[-\frac{a}{2} \cdot \frac{m(\Lambda)}{\Lambda^2 \ln \Lambda^2} - \frac{\sigma}{\Lambda^4} (\ln \Lambda^2)^{a/2-2} (\ln \Lambda^2 + 1 - a/2) \right] \\ &\simeq \frac{2}{6\pi^2 a C_2} \Lambda^2 (\ln \Lambda^2)^{a/2} \left[\frac{a}{2} \cdot \frac{m(\Lambda)}{\Lambda^2 \ln \Lambda^2} + \frac{\sigma}{\Lambda^4} (\ln \Lambda^2)^{a/2-1} \right]. \end{aligned} \tag{21}$$

We note that $m(\Lambda)$ is the bare quark mass defined at the scale Λ, as mentioned before, and the factor $(\ln \Lambda^2)^{a/2} m(\Lambda)$ in Eq. (21) is equal to $(\ln \kappa^2)^{a/2} m_R(\kappa)$ which is cutoff independent. [1] Hence, $F(\Lambda)$ vanishes in the continuum limit, provided σ remains finite in this limit. As concerns $F(0)$, it turns out to be

$$\begin{aligned} F(0) &= \frac{2}{3C_2} \left[\Sigma(p_E) - m(\Lambda) \right] \\ &\quad \times \frac{(p_E^2)^2}{p_E^2 d\bar{g}^2(p_E)/dp_E^2 - \bar{g}^2(p_E)} \frac{d\Sigma(p_E)}{dp_E^2} \Bigg|_{p_E=0}. \end{aligned} \tag{22}$$

Since we will introduce an infrared finite running coupling and mass function in Eqs. (34) and (35), we can set $F(0) = 0$.

After all, in the continuum limit, we get $V_S = 0$ and the modified version of the CJT effective potential becomes

$$\begin{aligned} V[\Sigma(p_E)] &= -2 \int \frac{d^4 p_E}{(2\pi)^4} \, \ln \frac{\Sigma^2(p_E) + p_E^2}{p_E^2} \\ &\quad - \frac{2}{3C_2} \int dp_E^2 \, \frac{1}{\Delta(p_E)} \left(\frac{d}{dp_E^2} \Sigma(p_E) \right)^2. \end{aligned} \tag{23}$$

---

[1] In this paper, we use the mass-independent renormalization scheme [24,25]. In this scheme, all the renormalization constants are fixed by massless theory. The bare quark mass $m(\Lambda)$ and the renormalized mass $m_R(\kappa)$ at the renormalization point κ are related as

$$m(\Lambda) = Z_S^{-1}(\Lambda, \kappa) m_R(\kappa)$$

where $Z_S^{-1}(\Lambda, \kappa)$ is the renormalization constant for the composite operator $\bar{q}q$:

$$\begin{aligned} (\bar{q}q)_R &= Z_S^{-1} \cdot (\bar{q}q)_\Lambda, \\ Z_S^{-1}(\Lambda, \kappa) &= \left(\frac{\ln \kappa^2}{\ln \Lambda^2} \right)^{a/2}. \end{aligned}$$

A few comments are in order.

(1) The extremum condition for $V[\Sigma(p_E)]$ in Eq. (23) with respect to $\Sigma(p_E)$ leads to Eq. (11) which is equivalent to the original equation (8) in the Higashijima-Miransky approximation apart from the two boundary conditions. We will take account of these conditions when we introduce the trial mass function.

(2) Even if chiral symmetry is explicitly broken, we do not use the condition adopted in Ref. [23]. Instead, our condition is $V_S = 0$ (see Eq. (17)).

The relation between σ and the quark condensate is as follows. The renormalization group invariant vacuum expectation value of $\bar{q}q$ is given by

$$\begin{aligned}\langle\bar{q}q\rangle &= \langle 0|(\bar{q}q)_R|0\rangle(\ln\kappa^2)^{-a/2} \\ &= \lim_{\Lambda\to\infty}\langle 0|(\bar{q}q)_\Lambda|0\rangle(\ln\Lambda^2)^{-a/2} \\ &= \lim_{\Lambda\to\infty} G(\Lambda),\end{aligned} \tag{24}$$

where $G(\Lambda)$ is defined as

$$G(\Lambda) = Z^{-1}(\Lambda)(-4N_c)\int^\Lambda \frac{d^4p_E}{(2\pi)^4}\ \frac{\Sigma(p_E)}{\Sigma^2(p_E)+p_E^2}, \tag{25}$$

with

$$Z(\Lambda) = (\ln\Lambda^2)^{a/2}. \tag{26}$$

Using Eq. (11), $G(\Lambda)$ is rewritten as

$$G(\Lambda) = -Z^{-1}(\Lambda)\frac{4N_c}{3C_2}\int_0^{\Lambda^2} dp_E^2 \frac{d}{dp_E^2}\left(\frac{1}{\Delta(p_E)}\frac{d\Sigma(p_E)}{dp_E^2}\right). \tag{27}$$

This expression is convenient to isolate the ultraviolet divergence as the RHS is linear in $\Sigma(p_E)$. Using Eqs. (19) and (20), as can be verified by direct calculation, $G(\Lambda)$ is obtained as

$$G(\Lambda) = m(\Lambda)I_p(\Lambda) + \sigma I_n(\Lambda), \tag{28}$$

where the lower bound in the definite integral automatically vanishes by the same argument as given for $F(0)$ and a perturbative contribution $I_p(\Lambda)$ and a nonperturbative one $I_n(\Lambda)$ are given as follows:

$$I_p(\Lambda) = -\frac{N_c}{3\pi^2 C_2}\Lambda^2(\ln\Lambda^2)^{-a/2}, \tag{29}$$

$$I_n(\Lambda) = -\frac{2N_c}{3\pi^2 a C_2}. \tag{30}$$

As discussed in Ref. [16,17], the perturbative contribution is quadratically divergent. We are interested in the purely nonpertubetive effect; therefore, we simply subtract the perturbative effect from Eq. (28) and re-define the quark condensate as

$$\begin{aligned}\langle\bar{q}q\rangle &\equiv \sigma I_n(\Lambda) \\ &= -\frac{3}{2\pi^2 a}\sigma.\end{aligned} \tag{31}$$

The relation between σ and $\langle\bar{q}q\rangle$ is the same as in the massless theory. We do not use Eq. (24) but Eq. (31) to extract $\langle\bar{q}q\rangle$ from σ_{min}, the location of a minimum of the effective potential. Consequently, the asymptotic behavior of the mass function in the continuum limit takes the following form

$$\Sigma(p_E) \to m_R(\ln p_E^2)^{-a/2} - \langle\bar{q}q\rangle\frac{2\pi^2 a}{3p_E^2}(\ln p_E^2)^{a/2-1}, \tag{32}$$

where

$$m_R = m_R(\kappa)(\ln\kappa^2)^{a/2} = \lim_{\Lambda\to\infty} m(\Lambda)(\ln\Lambda^2)^{a/2} \tag{33}$$

is the renormalization group invariant quark mass. This asymptotic behavior is completely coincident with that obtained by using the operator product expansion and the renormalization group equation [26]. Notice that in these arguments there are no ambiguities in separating the perturbative and the nonperturbative contribution in $\langle\bar{q}q\rangle$.

Now we are in a position to introduce a modified running coupling and a trial mass function. We use the following modified running coupling [21]

$$\bar{g}^2(p_E) = \frac{2\pi^2 a}{\ln(p_E^2 + p_R^2)}, \tag{34}$$

where p_R is a parameter to regularize the divergence of the QCD running coupling at $p_E = 1(\Lambda_{\rm QCD})$. This modified running coupling approximately develops according to the QCD renormalization group equation of one-loop order at large p_E^2, while it smoothly approaches a constant as p_E^2 decreases.

Corresponding to the above running coupling, the SDE with the two boundary conditions suggests the following trial mass function

$$\Sigma(p_E) = m_R[\ln(p_E^2 + p_R^2)]^{-a/2} + \frac{\sigma}{p_E^2 + p_R^2}[\ln(p_E^2 + p_R^2)]^{a/2-1}. \tag{35}$$

The trial mass function is infrared finite, and moreover, it has the same asymptotics as in Eq. (32).

When we also consider the pseudoscalar degree of freedom in the effective potential, we expand the full quark propagator in Minkowski space as follows

$$iS^{-1}(p) = \gamma\cdot p - \Sigma(p) - i\gamma_5\Sigma_5(p). \tag{36}$$

An effective potential for this case is obtained straightforwardly as

$$\begin{aligned} V[\Sigma(p_E),\Sigma_5(p_E)] = &-2\int\frac{d^4p_E}{(2\pi)^4}\ \ln\frac{\Sigma^2(p_E)+\Sigma_5^2(p_E)+p_E^2}{p_E^2} \\ &-\frac{2}{3C_2}\int dp_E^2\ \frac{1}{\Delta(p_E)}\left[\left(\frac{d}{dp_E^2}\Sigma(p_E)\right)^2+\left(\frac{d}{dp_E^2}\Sigma_5(p_E)\right)^2\right]. \end{aligned} \tag{37}$$

The mass function $\Sigma_5(p_E)$ satisfies the SDE which has the form as in Eq. (11) where the bare quark mass is set zero. Therefore the trial mass function for $\Sigma_5(p_E)$ should be

$$\Sigma_5(p_E) = \frac{\sigma_5}{p_E^2 + p_R^2}[\ln(p_E^2 + p_R^2)]^{a/2-1}, \tag{38}$$

where $\sigma_5 = 2\pi^2 a\langle\bar{q}i\gamma_5 q\rangle/3$. However, except when we consider a mass of pseudoscalar boson we can put $\Sigma_5(p_E) = 0$ without loss of generality.

Substituting Eqs. (34) and (35) into Eq. (23), we have the following expression for the effective potential

$$\begin{aligned} V(\sigma;m_R) = &-\frac{2}{(4\pi)^2}\int_{t_R}^{\infty}dt\ e^t(e^t-e^{t_R})\ln\frac{e^t-e^{t_R}+(m_R t^{-a/2}+\sigma t^{a/2-1}e^{-t})^2}{e^t-e^{t_R}+m_R^2 t^{-a}} \\ &+\frac{m_R\sigma}{4\pi^2}\int_{t_R}^{\infty}dt\ \frac{e^{-t}(e^t-e^{t_R})^2(t+1-a/2)}{t(e^t-e^{t_R}+te^t)} \\ &+\frac{9}{32\pi^2}\sigma^2\int_{t_R}^{\infty}dt\ \frac{(1-e^{t_R-t})^2(t+1-a/2)^2}{t^{2-a}(e^t-e^{t_R}+te^t)}, \end{aligned} \tag{39}$$

where we made the change of the integration variable

$$t = \ln(p_E^2 + p_R^2)\ \ ,\ \ t_R = \ln(p_R^2), \tag{40}$$

and subtracted the σ independent term which is exponentially divergent in t. The infrared regularization parameter t_R specifies the coupling constant in the low energy region. Indeed, $\bar{g}^2(0) = 2\pi^2 a/t_R$ is proportional to the inverse of t_R. We note that in the first two terms in Eq. (39) there are logarithmic divergences in t which cancel out each other. This is because the fact that we take into account the correct renormalization group effects in $\bar{g}^2(p_E)$ and in $\Sigma(p_E)$ [23].

Before we turn to the effective potential at finite temperature and density, we examine some numerical consequences of Eq. (39) and make a comparison with the results by other authors. Figure 1 shows the t_R dependence of $\langle\bar{q}q\rangle$ in

the chiral limit. Chiral symmetry is broken for relatively small t_R whereas it is restored for large t_R. Notice that $\langle\bar{q}q\rangle$ is stable under the change of t_R if $t_R < 0.4$ and the critical value of t_R is $(t_R)_{critical} \simeq 0.56$. This critical value of t_R is about one third of that obtained in Ref. [21] in which the SDE with the same running coupling has been solved. In our model,

$$\begin{aligned}(\alpha_s)_{critical} &= \frac{2\pi^2 a}{(t_R)_{critical}} \\ &\simeq 3\cdot\frac{\pi}{3C_2},\end{aligned} \tag{41}$$

where $\pi/(3C_2)$ is the critical value obtained from the SDE analysis in Ref. [21] and also in quenched QED_4 with the replacement α by $C_2\alpha$ [16]. We note that, in Ref. [19,21], it has been shown that the $(\alpha_s)_{critical}$ obtained by using the CJT effective potential (6) and (7) is about two times of $\pi/(3C_2)$. These differences may arise from the fact that, in the framework of the variational approach, we restricted the class of trial function and we used the modified form of the CJT effective potential.

Figure 2 shows the plot of the quark condensate $\langle\bar{q}q\rangle$ versus quark mass m_R analogous to the relation between the spontaneous magnetization of the ferro-magnetism and the external magnetic field. The curves show the cases $t_R = 0.1$ and $t_R = 0.8$. When t_R is sufficiently small, i.e., the coupling constant in low energy region is sufficiently large, the quark condensate discontinuously changes its sign at $m_R = 0$. This is a clear evidence of the dynamical chiral symmetry breaking. On the other hand, when t_R is sufficiently large, the discontinuity of the quark condensate disappears.

The chiral phase, even at zero temperature and density, depends on the number of massless flavors. At some value of n_f (less than $11N_c/2$), a phase transition to the chirally symmetric phase is expected. In Ref. [27], it has been argued that, in connection with the infrared fixed point in the two-loop β function, there exists a critical number of fermions n_f^c, above which there is no chiral symmetry breaking. Figure 3 shows the t_R dependence of n_f^c, where n_f^c is considered as a continuous number. For $t_R = 0.1$ our model suggests that $n_f^c = 10$, and this result is consistent with lattice QCD results [28] which gives $8 < n_f^c \leq 12$ (see also Ref. [27]).

B. Effective potential at finite temperature and density

In this subsection we discuss the effective potential at finite temperature and density. In order to calculate the effective potential at finite temperature and density we apply the imaginary time formalism [29]

$$\int\frac{dp_4}{2\pi}f(p_4) \to T\sum_{n=-\infty}^{\infty} f(\omega_n + i\mu), \tag{42}$$

where $\omega_n = (2n+1)\pi T$ $(n = 0, \pm1, \pm2, \cdots)$ is the fermion Matsubara frequency and μ represents the quark chemical potential. In addition, we need to define the running coupling and the trial mass function at finite temperature and density. We adopt the following functions for $\mathcal{D}_{T,\mu}(p)$, $\Sigma_{T,\mu}(p)$ and $\Sigma_{5;T,\mu}(p)$ by replacing p_4 in $\mathcal{D}(p_E)$, $\Sigma(p_E)$ and $\Sigma_5(p_E)$ with ω_n:

$$\mathcal{D}_{T,\mu}(p) = \frac{2\pi^2 a}{\ln(\omega_n^2 + |\vec{p}|^2 + p_R^2)}\,\frac{1}{\omega_n^2 + |\vec{p}|^2}, \tag{43}$$

$$\begin{aligned}\Sigma_{T,\mu}(p) &= m_R\left[\ln(\omega_n^2 + |\vec{p}|^2 + p_R^2)\right]^{-a/2} \\ &\quad + \frac{\sigma}{\omega_n^2 + |\vec{p}|^2 + p_R^2}\left[\ln(\omega_n^2 + |\vec{p}|^2 + p_R^2)\right]^{a/2-1},\end{aligned} \tag{44}$$

$$\Sigma_{5;T,\mu}(p) = \frac{\sigma_5}{\omega_n^2 + |\vec{p}|^2 + p_R^2}\left[\ln(\omega_n^2 + |\vec{p}|^2 + p_R^2)\right]^{a/2-1}. \tag{45}$$

In Eq. (43) we do not introduce the μ dependence in $\mathcal{D}_{T,\mu}(p)$. The gluon momentum squared is the most natural argument of the running coupling at zero temperature and density, in the light of the chiral Ward-Takahashi identity [30,31]. Then it is reasonable to assume that $\mathcal{D}_{T,\mu}(p)$ does not depend on the quark chemical potential. In addition, the screening mass is not included in Eq. (43). We comment on this point in Sec. IV.

As concerns the mass function, we use the same function as Eqs. (35) and (38) except that we replace p_4 with ω_n. As already noted in Sec. II A, the quark wave function does not suffer the renormalization in the Landau gauge for

$T = \mu = 0$, while, the same does not hold for finite temperature and/or density. However, we assume that the wave function renormalization is not required even at finite temperature and/or density, for simplicity.

Furthermore, we neglect the T-μ dependent terms in the quark and gluon propagators which arise from the perturbative expansion. We expect that the phase structure is not so affected by these approximations.

Using Eqs. (43), (44) and (45), it is easy to write down the effective potential $V(\sigma, \sigma_5; m_R)$ (see Appendix). Even at finite temperature and/or density, we determine the value of $\langle \bar{q}q \rangle$ through $\langle \bar{q}q \rangle = -(3/2\pi^2 a)\sigma_{min}$ where σ_{min} is the location of the minimum of $V(\sigma, \sigma_5; m_R)$.

III. CHIRAL PHASE TRANSITION AT HIGH TEMPERATURE AND DENSITY:NUMERICAL RESULTS

In numerical calculation, as mentioned before, we put $N_c = n_f = 3$. Furthermore, since it was known that the temperature and chemical potential dependence of the quantities such as $\langle \bar{q}q \rangle$ and f_π are stable under the change of the infrared regularization parameter [11], in the first place, we fix $t_R = 0.1$ and determine the value of $\Lambda_{\rm QCD}$ by the condition $f_\pi = 93$ MeV at $T = \mu = 0$ and $m_R = 0$. In this case, the pion decay constant is approximately given by [32]

$$f_\pi^2 = 4N_c \int \frac{d^4 p_E}{(2\pi)^4} \frac{\Sigma(p_E)}{[\Sigma^2(p_E) + p_E^2]^2} \left(\Sigma(p_E) - \frac{p_E^2}{2} \frac{d\Sigma(p_E)}{dp_E^2} \right), \tag{46}$$

and we have $\Lambda_{\rm QCD} = 738$ MeV. Secondly, we assume the light quarks (u and d) are degenerate in mass and take the quark mass evaluated at $\kappa = 1$ GeV as

$$m_R(1\text{GeV}) = \frac{m_u(1\text{GeV}) + m_d(1\text{GeV})}{2} = 7\text{MeV}. \tag{47}$$

With Eq. (33) the renormalization group invariant quark mass m_R extracted from the above-mentioned value becomes

$$m_R = 7.6 \times 10^{-3} \Lambda_{\rm QCD}. \tag{48}$$

A. $T \neq 0, \mu = 0$ case

The phase diagram in the chiral limit is shown in Fig. 4. We have found second-order phase transition, with the critical temperature $T_c = 129$ MeV for $\mu = 0$ [15].

Figure 5 shows the temperature dependence of the effective potential at $\mu = 0$ for $m_R(1\text{GeV}) = 7$ MeV. We can realize that σ_{min} the minimum of the effective potential continuously approaches to the origin as temperature increases. Figure 6 shows the temperature dependence of σ_{min} for the chiral limit and the case $m_R(1\text{GeV}) = 7$ MeV. Below T_c, the two curves are almost the same apart from the small difference in their magnitude. On the other hand, above T_c, while $\sigma_{\rm min}$ remains nonzero for $m_R(1\text{GeV}) = 7$ MeV, the one in the chiral limit vanishes. In other words, the temperature dependence of the order parameter is dominated by the dynamical symmetry breaking in low-T region, whereas by explicit breaking in high-T region.

Let us examine the critical exponents. Assuming the mean-field expansion, we expand V as follows

$$V = a_2(T)\sigma^2 + a_4(T)\sigma^4 + b(T) m_R \sigma + \cdots, \tag{49}$$

where ellipsis represents higher order contributions in m_R and σ that is expected to be small near T_c and the critical temperature is determined by the condition $a_2(T_c) = 0$ for $m_R = 0$. The three critical exponents β, γ and δ are defined as follows

$$\langle \bar{q}q \rangle|_{m_R=0} \simeq \left(1 - \frac{T}{T_c}\right)^{\beta}, \tag{50}$$

$$\left. \frac{\partial \langle \bar{q}q \rangle}{\partial m_R} \right|_{m_R=0} \simeq \left(1 - \frac{T}{T_c}\right)^{-\gamma}, \tag{51}$$

$$\langle \bar{q}q \rangle|_{T=T_c} \simeq m_R^{1/\delta}, \tag{52}$$

where $T < T_c$. Since we have confirmed that, except for $a_2(T)$, all the coefficients in Eq. (49) do not have singular behavior near T_c we can define the exponent γ, instead of Eq. (51), as

$$a_2(T) \simeq \left(1 - \frac{T}{T_c}\right)^{\gamma}. \tag{53}$$

These critical exponents are determined numerically by the use of the linear log fit, for instance,

$$\ln\langle\bar{q}q\rangle|_{m_R=0} = \beta \ln\left(1 - \frac{T}{T_c}\right) + C, \tag{54}$$

where C is independent of T. In order to determine the exponent we use the χ^2 fitting (see Figs. 7 and 8). The results are

$$\beta \simeq 0.5\ ,\ \gamma \simeq 1\ ,\ \delta \simeq 3. \tag{55}$$

Therefore, our results confirm the Landau theory of the second-order phase transition, i.e., a second-order phase transition with the classical mean-field values for the critical exponents, and coincident with that obtained in Ref. [33].

In order to calculate the masses of the scalar (σ) and pseudoscalar (π) bosons, we include the pseudoscalar degree of freedom in V and take the second derivative. The values of masses are obtained by multiplying the second derivative by the appropriate factor f:

$$M_\sigma^2 = f\frac{\partial^2 V}{\partial\sigma^2}\bigg|_{\rm min}\ ,\ M_\pi^2 = f\frac{\partial^2 V}{\partial\sigma_5^2}\bigg|_{\rm min}. \tag{56}$$

Here, "min" at the end of the equations means that they are evaluated at the minimum of $V(\sigma, \sigma_5; m_R)$. In this paper, we do not examine the factor f; rather, we study the "mass ratio" M_σ/M_π. As discussed in Refs. [34,35], below T_c, $M_\pi(T)$ weakly depends on the temperature and the value is dominated by the current quark mass and for $T \geq T_c$ the pion loses its Goldstone nature. On the other hand, $M_\sigma(T)$ decreases in association with the partial restoration of chiral symmetry. Therefore, above some temperature T^*, $M_\sigma(T)$ becomes smaller than $2M_\pi(T)$ and the width $\Gamma_{\sigma\to 2\pi} \propto \sqrt{1 - 4M_\pi^2/M_\sigma^2}$ vanishes. Figure 9 shows the temperature dependence of M_σ/M_π. We evaluate T^* and find

$$T^* \simeq 0.97 T_c. \tag{57}$$

If we fix the $M_\pi(T = 0)$ to 140 MeV, then, $M_\sigma(T = 0)$ turns out to be 668 MeV. The temperature dependence of M_σ and M_π is shown in Fig. 10.

B. $T = 0, \mu \neq 0$ case

Figure 11 shows the chemical potential dependence of the effective potential at $T = 0$ for $m_R(1\text{GeV}) = 7$ MeV. In the chiral limit, the critical chemical potential is $\mu_c = 422$ MeV. We note that, in $m_R(1\text{GeV}) = 7$ MeV case, another extremum appears for relatively larger value of μ. Figure 12 shows the μ dependence of σ_{min}. The quark condensate discontinuously vanishes at $\mu = \mu_c$ in the chiral limit, indicating the first order phase transition. In $m_R(1\text{GeV}) = 7$ MeV case, σ_{min} changes discontinuously at $\mu = \mu_c^*$, a little larger value than μ_c. However, because of finite quark mass, it does not vanish for $\mu > \mu_c^*$. It is widely expected that as m_R, namely the external field, grows the discontinuity weakens or disappears. We examined up to $m_R \simeq 400$ MeV, however, the discontinuity does not vanish.

C. $T \neq 0, \mu \neq 0$ case

Figure 13 shows the μ dependence of σ_{min} for several temperatures. We expect that there is the critical end point E, where the discontinuous jump of the order parameter ends in the T-μ plane. Apparently its position is

$$T_E \sim 100\ \text{MeV},\ \mu_E \sim 300\ \text{MeV}, \tag{58}$$

though it is not easy to determine accurately. The physics near the critical end point is interesting in the light of relativistic heavy-ion collision experiments [37]. This, however, is beyond the scope of this work.

IV. SUMMARY AND DISCUSSION

The primary purpose of this paper was to study the current quark mass effects on chiral phase transition of QCD in the improved ladder approximation. We made use of the CJT effective potential because the use of the SDE only is not adequate for studying the phase transition, and moreover, it was known that, in studies of the SDE, there is a difficulty in removing the perturbative contribution from the quark condensate [16,17].

To begin with, we modified the form of the CJT effective potential using the two representations of the SDE. We then studied the t_R and m_R dependence of the order parameter and obtained the reasonable results. Being motivated by Ref. [27], the critical number of massless flavors was also studied. Our result is consistent with lattice QCD results for relatively small t_R. Incidentally, our formulation of the effective potential is entirely based on the Higashijima-Miransky approximation. However it was known that the chiral Ward-Takahashi identity is broken unless gluon momentum squared is used as the argument of the running coupling [30]. Therefore, it is desirable to formulate the effective potential for the finite current quark mass independently of the Higashijima-Miransky approximation.

We then extended the effective potential to finite temperature and density by introducing the functions $\mathcal{D}_{T,\mu}(p)$, $\Sigma_{T,\mu}(p)$ and $\Sigma_{5;T,\mu}(p)$. We calculated the effective potential numerically and investigated current quark mass effects on the chiral phase structure. In either $T \neq 0$, $\mu = 0$ or $T = 0$, $\mu \neq 0$ case, the behavior of the order parameter in low-T or low-μ region does not suffer the effects of finite, however small enough, current quark mass. On the other hand, in high-T or high-μ region its behavior is perfectly dominated by the current quark mass. We also examined numerically the critical exponents β, γ and δ and confirmed the Landau theory of the second-order phase transition. The temperature dependence of the mass ratio M_σ/M_π was also studied. We found that for $T > T^* = 0.97T_c$ the mass ratio becomes smaller than two. In Ref. [35,38], the temperature T^* has been obtained and our results are almost coincident with theirs. We note that the similar temperature dependence of the mass ratio have been also obtained from the Nambu–Jona-Lasinio model [34] and the linear sigma model [39]. In the previous paper [15], in the chiral limit, we found the tricritical point at $T_P = 107$ MeV, $\mu = 210$ MeV. We found ,in $m_R(1\text{GeV}) = 7$ MeV case, the position of the critical end point is $T_E \sim 100$ MeV, $\mu_E \sim 300$ MeV.

Finally, some comments are in order. The treatment of the quark and gluon propagator at finite temperature and density is somewhat oversimplified in the present work. In the future, we would like to consider the wave function renormalization and more appropriate functional form for $\Sigma_{T,\mu}(p)$, $\Sigma_{5;T,\mu}(p)$ and $\mathcal{D}_{T,\mu}(p)$ which would depend on T and μ explicitly. In particular, we should take into account the screening of the gluon in $\mathcal{D}_{T,\mu}(p)$, that is to say, the effects of the Debye (electric) mass and the nonperturbative magnetic mass, which arises from the dimensional reduction, $m_{mag} \sim g^2T$ at $T \neq 0$ [36]. They may affect the precise location of the critical line. We also note that these screening masses are probably related to the infrared regularization parameter p_R, though it is not easy to show it explicitly. Furthermore, it is well known that gauge covariance is lost, namely the Ward-Takahashi identity for the fermion–gauge-boson vertex is not satisfied when one uses the ladder approximation. Of course, gauge invariance in the case of the non-Abelian gauge theory is ensured by the Slavnov-Taylor identity which, in covariant gauges, includes a contribution connected with the Faddeev-Popov ghost fields. Thus, addressing ourselves to gauge covariance in QCD is difficult, however, progress has been made with the Abelian gauge theory [16]. Although we suppose that results of the analysis will be essentially unchanged, it is preferable to use the correct form of the fermion–gauge-boson vertex. As concerns the phase structure, it is interesting to study the physics near the critical end point, for example, critical slowing down [37]. We also plan to study the quark pairing including a color superconductivity and a "color-flavor locking" [5] (for $N_c = N_f = 3$ case).

ACKNOWLEDGMENTS

O.K. would like to thank V. A. Miransky for useful discussions and for reading the manuscript.

APPENDIX:

In this appendix, we show the effective potential $V(\sigma, \sigma_5; m_R)$ explicitly. In the first place, we consider the case of zero temperature and finite chemical potential.

Using Eqs. (44) and (45), we obtain

$$V_1(\sigma,\sigma_5;m_R) = -2\int \frac{d^4p_E}{(2\pi)^4}\ \ln\frac{\Sigma^2_{T,\mu}(p)+\Sigma^2_{5;T,\mu}(p)+(p_4+i\mu)^2+|\vec{p}|^2}{(p_4+i\mu)^2+|\vec{p}|^2}$$
$$= -\frac{1}{4\pi^3}\int_p \ln\left[\frac{(\Sigma^2_{T,\mu}(p)+\Sigma^2_{5;T,\mu}(p)+p_4^2+|\vec{p}|^2-\mu^2)^2+(2\mu p_4)^2}{(p_4^2+|\vec{p}|^2-\mu^2)^2+(2\mu p_4)^2}\right]$$
$$+\delta^{(1)}, \tag{A1}$$

where the imaginary part of V_1 is odd function of p_4; therefore it has been removed from Eq. (A1) and

$$\int_p = \int_{-\infty}^{\infty} dp_4 \int_0^{\infty} d|\vec{p}|\ |\vec{p}|^2. \tag{A2}$$

Moreover, in order to remove the divergence, we introduce $\delta^{(1)} = V_1(0,0;m_R)$ the term independent of σ and σ_5.

In Eq. (37), we carry out the momentum differentiation and, then, use the Eqs. (43), (44) and (45). V_2 is obtained as

$$V_2(\sigma,\sigma_5;m_R) = \frac{4}{3C_2a\pi^3}\int_p \frac{(p_4^2+|\vec{p}|^2)^2(p_4^2+|\vec{p}|^2+p_R^2)[\ln(p_4^2+|\vec{p}|^2+p_R^2)]^2}{(p_4^2+|\vec{p}|^2+p_R^2)\ln(p_4^2+|\vec{p}|^2+p_R^2)+p_4^2+|\vec{p}|^2}\mathcal{S}^2(p;\sigma,m_R)$$
$$+\frac{4\sigma_5^2}{3\pi^3C_2a}\int_p \frac{(p_4^2+|\vec{p}|^2)^2[\ln(p_4^2+|\vec{p}|^2+p_R^2)]^{a-2}}{(p_4^2+|\vec{p}|^2+p_R^2)\ln(p_4^2+|\vec{p}|^2+p_R^2)+p_4^2+|\vec{p}|^2}$$
$$\times\frac{\left[\ln(p_4^2+|\vec{p}|^2+p_R^2)+1-a/2\right]^2}{(p_4^2+|\vec{p}|^2+p_R^2)^3}$$
$$+\delta^{(2)}, \tag{A3}$$

where the function

$$\mathcal{S}(p;\sigma,m_R) = -\frac{am_R}{2}\frac{\left[\ln(p_4^2+|\vec{p}|^2+p_R^2)\right]^{-a/2-1}}{p_4^2+|\vec{p}|^2+p_R^2}$$
$$-\frac{\sigma}{(p_4^2+|\vec{p}|^2+p_R^2)^2}\left[\ln(p_4^2+|\vec{p}|^2+p_R^2)\right]^{a/2-2}\left[\ln(p_4^2+|\vec{p}|^2+p_R^2)+1-\frac{a}{2}\right], \tag{A4}$$

is introduced and $\delta^{(2)} = V_2(0,0;m_R)$ is again the subtraction term independent of σ and σ_5.

At finite temperature and chemical potential, the p_4 integration in Eqs. (A1) and (A3) is replaced by a sum over the fermion Matsubara frequency.

---

[1] For general reviews see, for example, J. Cleymans, R. V. Gavai, and E. Suhonen, Phys. Rep. **130**, 217 (1986); L. McLerran, Rev. Mod. Phys. **58**, 1021 (1986).

[2] B. Barrois, Nucl. Phys. B **129**, 390 (1977); "Nonpertubative effects in dense quark matter", Ph.D thesis, California Institute of Technology, Report No. UMI 79-04847-mc (1979); S. C. Frautschi, in Proceedings of the Workshop on Hadronic Matter at Extreme Energy Density, Erice, Italy, 1978, edited by N. Cabbibo (Plenum, New York, 1980); D. Bailin and A. Love, Phys. Rep. **107**, 325 (1984).

[3] M. Iwasaki and T. Iwado, Phys. Lett. B **350**, 163 (1995).

[4] M. Alford, K. Rajagopal, and F. Wilczek, Phys. Lett. B **422** , 247 (1998); J. Berges and K. Rajagopal, Nucl. Phys. B **538**, 215 (1999); R. Rapp, T. Schäfer, E. V. Shuryak, and M. Velkovsky, Phys. Rev. Lett. **81**, 53 (1998); T. Schäfer and F. Wilczek, Phys. Rev. D **60**, 114033 (1999); R. D. Pisarski and D. H. Rischke, Phys. Rev. D **61**, 051501 (2000); *ibid.* **61**, 074017 (2000); D. K. Hong, V. A. Miransky, I. A. Shovkovy, and L. C. R. Wijewardhana, Phys. Rev. D **61**, 056001 (2000); W. E. Brown, J. T. Liu, and H-c. Ren, Phys. Rev. D **61**, 114012 (2000); D. H. Hsu and M. Schwetz, Nucl. Phys. B **572**, 211 (2000).

[5] M. Alford, K. Rajagopal, and F. Wilczek, Nucl. Phys. B **537**, 443 (1999); T. Schäfer, Nucl. Phys. B **575**, 269 (2000); I. Shovkovy and L. C. R. Wijewardhana, Phys. Lett. B **470**, 189 (1999).

[6] D. Bailin, J. Cleymans, and M. D. Scadron, Phys. Rev. D **31**, 164 (1985).

[7] A. Kocić, Phys. Rev. D **33**, 1785 (1986).

[8] T. Akiba, Phys. Rev. D **36**, 1905 (1987).
[9] T. S. Evans and R. J. Rivers, Z. Phys. C **40**, 293 (1988).
[10] A. Barducci, R. Casalbuoni, S. De Curtis, R. Gatto, and G. Pettini, Phys. Rev. D **41**, 1610 (1990); Phys. Lett. B **240**, 429 (1990); Phys. Rev. D **46**, 2203 (1992); A. Barducci, R. Casalbuoni, G. Pettini, and R. Gatto, Phys. Rev. D **49**, 426 (1994).
[11] Y. Taniguchi and Y. Yoshida, Phys. Rev. D **55**, 2283 (1997).
[12] D. Blaschke, C. D. Roberts, and S. Schmidt, Phys. Lett. B **425**, 232 (1998); A. Bender, G. I. Poulis, C. D. Roberts, S. Schmidt, and A. W. Thomas, Phys. Lett. B **431**, 263 (1998); P. Maris, C. D. Roberts, and S. Schmidt, Phys. Rev. C **57**, R2821 (1998) ; C. D. Roberts and S. Schmidt, Prog. Part. Nucl. Phys. 45S1, 1 (2000).
[13] O. Kiriyama, M. Maruyama, and F. Takagi, Phys. Rev. D **58**, 116001 (1998).
[14] M. Harada and A. Shibata, Phys. Rev. D **59**, 014010 (1998).
[15] O. Kiriyama, M. Maruyama, and F. Takagi, Phys. Rev. D **62**, 105008 (2000).
[16] See, for example, V. A. Miransky, *Dynamical Symmetry Breaking in Quantum Field Theories* (World Scientific, Singapore, 1993); C. D. Roberts and A. G. Williams, Prog. Part. Nucl. Phys. **33**, 477 (1994).
[17] K. Kusaka, H. Toki, and S. Umisedo, Phys. Rev. D **59**, 116010 (1999).
[18] J. M. Cornwall, R. Jackiw, and E. Tomboulis, Phys. Rev. D **10**, 2428 (1974).
[19] K. Higashijima, Phys. Lett. B **124**, 257 (1983); P. Castorina and S-Y. Pi, Phys. Rev. D **31**, 411 (1985); V. P. Gusynin and Yu. A. Sitenko, Z. Phys. C **29**, 54 (1985).
[20] V. A. Miransky, Yad. Fiz. **38**, 468 (1983) [Sov. J. Nucl. Phys. **38**, 280 (1983)].
[21] K. Higashijima, Phys. Rev. D **29**, 1228 (1984); Prog. Theor. Phys. Suppl. **104**, 1 (1991).
[22] K-I. Aoki, M. Bando, T. Kugo, M. G. Mitchard, and H. Nakatani, Prog. Theor. Phys. **84**, 683 (1990).
[23] A. Barducci, R. Casalbuoni, S. De Curtis, D. Dominici, and R. Gatto, Phys. Rev. D **38**, 238 (1988).
[24] S. Weinberg, Phys. Rev. D **8**, 3497 (1973).
[25] G. 't Hooft, Nucl. Phys. B **61**, 455 (1973).
[26] H. D. Politzer, Nucl. Phys. B **117**, 397 (1976).
[27] T. Appelquist, J. Terning, and L. C. R. Wijewardhana, Phys. Rev. Lett. **77**, 1214 (1996); T. Appelquist, A. Ratnaweera, J. Terning, and L. C. R. Wijewardhana, Phys. Rev. D **58**, 105017 (1998).
[28] J. B. Kogut and D. K. Sinclair, Nucl. Phys. B **295**, 465 (1988); F. R. Brown, H. Chen, N. H. Christ, Z. Dong, R. D. Mawhinney, W. Schaffer, and A. Vaccarino, Phys. Rev. D **46**, 5655 (1992).
[29] See, for example, J. I. Kapusta, *Finite Temperature Field Theory* (Cambridge University Press, Cambridge, England, 1989).
[30] P. Jain and H. J. Munczek, Phys. Rev. D **44**, 1873 (1991).
[31] T. Kugo and M. G. Mitchard, Phys. Lett. B **282**, 162 (1992); *ibid.* **286**, 355 (1992).
[32] H. Pagels and S. Stoker, Phys. Rev. D **20**, 2947 (1979).
[33] A. Höll, P. Maris, and C. D. Roberts, Phys. Rev. C **59**, 1751 (1999).
[34] T. Hatsuda and T. Kunihiro, Phys. Lett. B **185**, 305 (1987); Prog. Theor. Phys. Suppl. **91**, 284 (1987); Phys. Rep. **247**, 221 (1994).
[35] A. Barducci, M. Modugno, G. Pettini, R. Casalbuoni, and R. Gatto, Phys. Rev. D **59**, 114024 (1999);A. Barducci, G. Pettini, R. Casalbuoni, and R. Gatto, *ibid.* **63**, 074002 (2001).
[36] D. J. Gross, R. D. Pisarski, and L. G. Yaffe, Rev. Mod. Phys. **53**, 43 (1981).
[37] B. Berdnikov and K. Rajagopal, Phys. Rev. D **61**, 105017 (2000);K. Rajagopal, Acta Phys. Polon. B **31**, 3021 (2000).
[38] P. Maris, C. D. Roberts, S. Schmidt, and P. C. Tandy, Phys. Rev. C **63**, 025202 (2001).
[39] H. -S. Roh and T. Matsui, Eur. Phys. J. A **1**, 205 (1998).

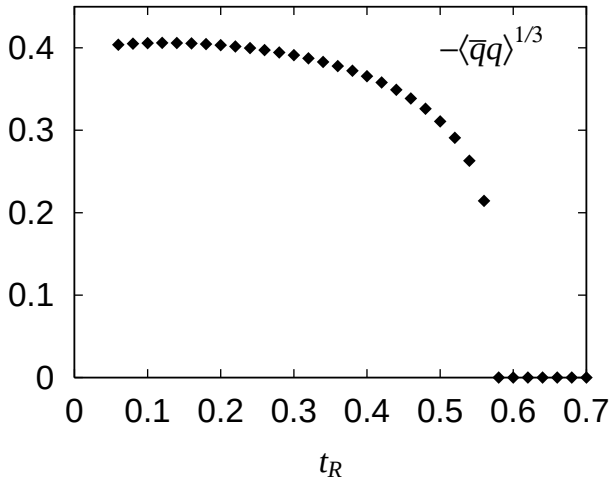

FIG. 1. The t_R dependence of $-\langle\bar{q}q\rangle^{1/3}$ in the chiral limit. The critical value of t_R is $(t_R)_{critical} = 0.56$. Notice that $-\langle\bar{q}q\rangle^{1/3}$ is taken to be dimensionless.

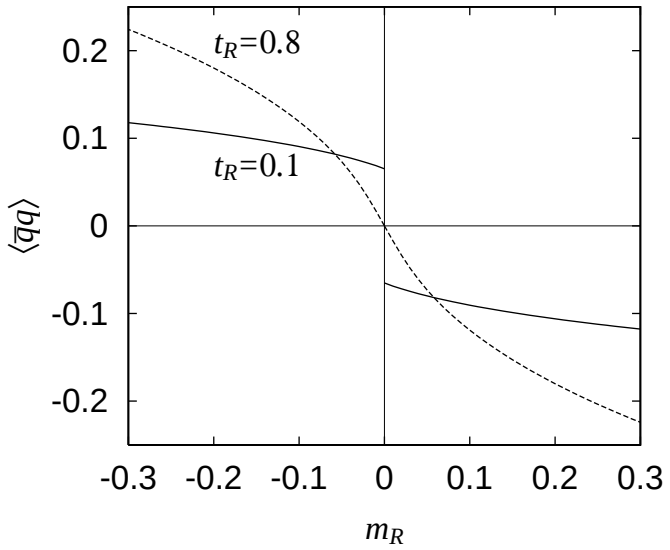

FIG. 2. The m_R dependence of $\langle\bar{q}q\rangle$ for the cases $t_R = 0.1$ (solid line) and $t_R = 0.8$ (dotted line). All the quantities are taken to be dimensionless.

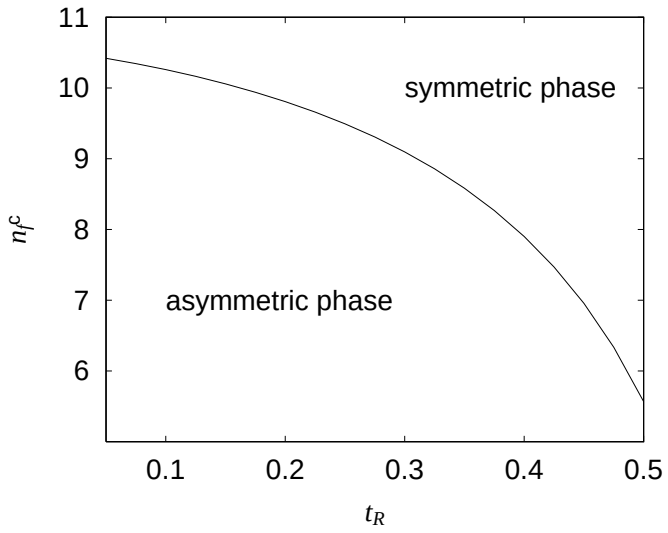

FIG. 3. The t_R dependence of n_f^c. n_f^c shows a tendency to decrease as t_R grows.

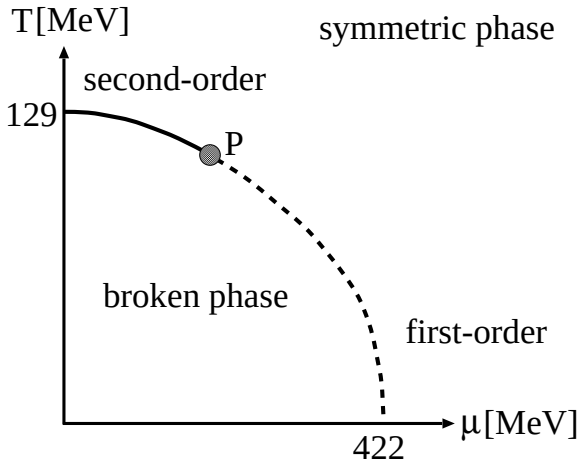

FIG. 4. Schematic view of the phase diagram obtained from our model in the chiral limit [15]. We have found a second-order transition at $T_c = 129$ MeV for $\mu = 0$ and a first-order one at $\mu_c = 422$ MeV for $T = 0$. Solid line indicates the phase transition of second-order and dashed line indicates that of first-order. A tricritical point P has been found at $T_P = 107$ MeV, $\mu_P = 210$ MeV.

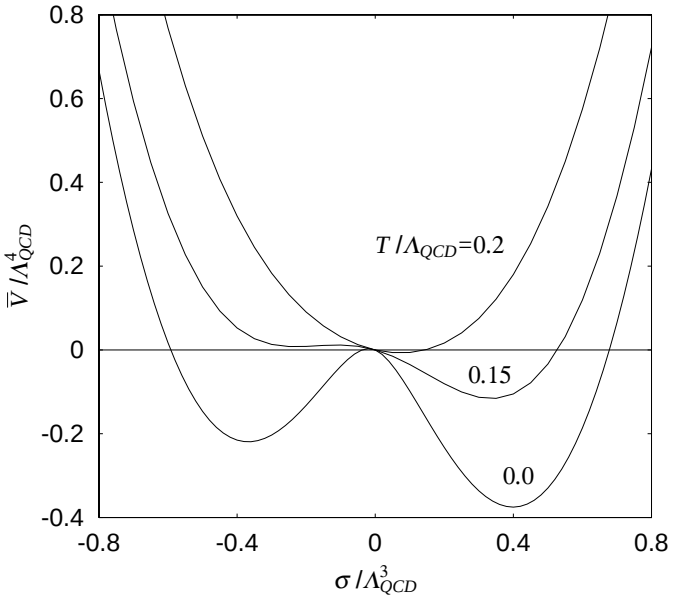

FIG. 5. The effective potential at finite temperature and zero chemical potential. $\overline{V}$ is defined by $\overline{V} = 24\pi^3 V$. The curves show the cases $T/\Lambda_{\rm QCD} = 0$, 0.15 and 0.2 with $m_R(1\text{GeV}) = 7$ MeV.

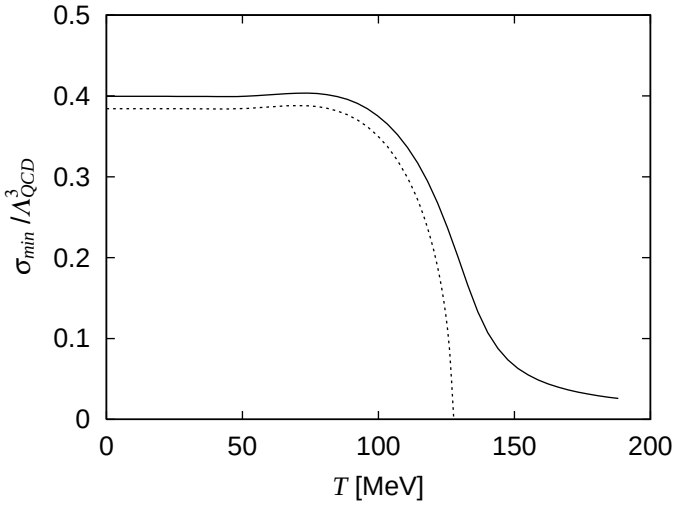

FIG. 6. The temperature dependence of σ_{min} at $\mu = 0$. The curves show the cases $m_R(1\text{GeV}) = 7$ MeV (solid line) and the chiral limit (dotted line).

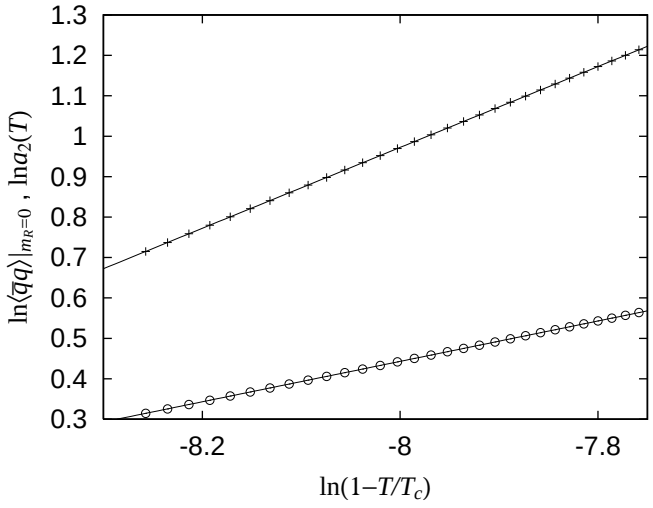

FIG. 7. Linear log fit to $\ln\langle\bar{q}q\rangle|_{m_R=0}$ (circle) and $\ln a_2(T)$ (plus). Here the absolute normalization of $\langle\bar{q}q\rangle|_{m_R=0}$ and $a_2(T)$ are taken arbitrary. The gradient of the linear function fitted the data for $\ln\langle\bar{q}q\rangle|_{m_R=0}$ and $\ln a_2(T)$ are $\beta = 0.4997$ and $\gamma = 1.000$, respectively.

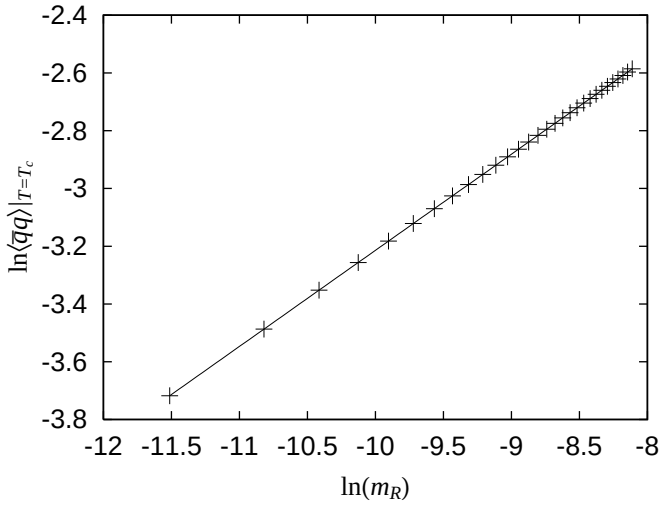

FIG. 8. Linear log fit to $\ln\langle\bar{q}q\rangle|_{T=T_c}$. The absolute normalization is taken arbitrary. The gradient of the linear function fitted the data is $1/\delta = 0.3329$.

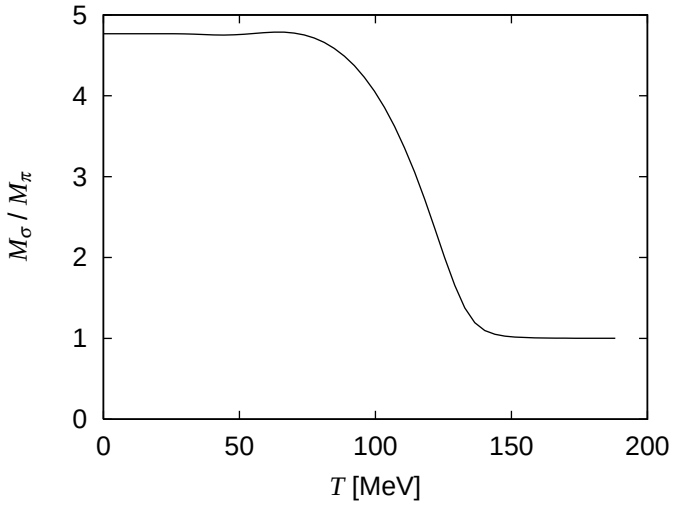

FIG. 9. The temperature dependence of the ratio M_σ/M_π.

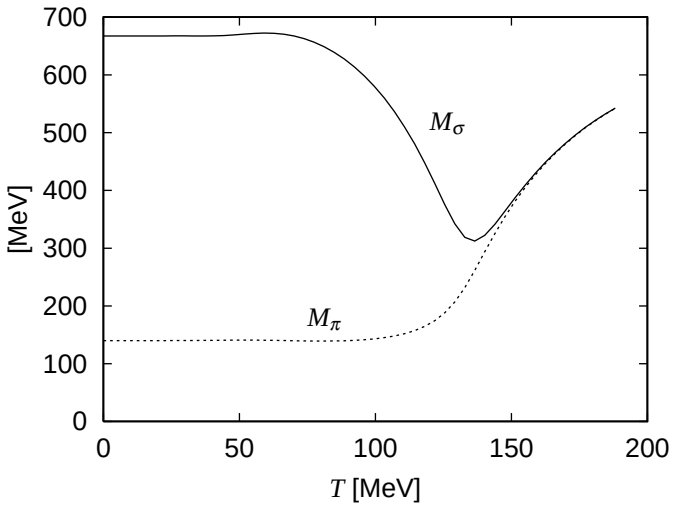

FIG. 10. The temperature dependence of M_σ (solid line) and M_π (dotted line).

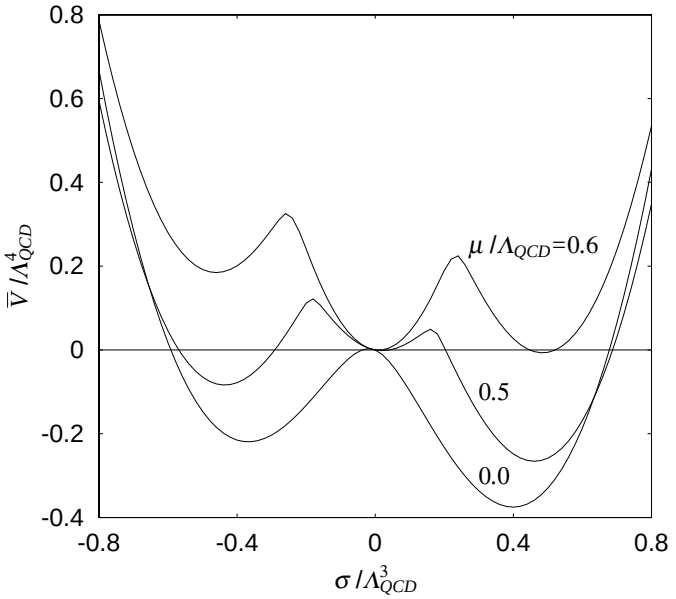

FIG. 11. The effective potential at finite chemical potential and zero temperature, where $\overline{V} = 24\pi^3 V$. The curves show the cases $\mu/\Lambda_{\rm QCD} = 0$, 0.5 and 0.6 with $m_R(1\text{GeV}) = 7$ MeV.

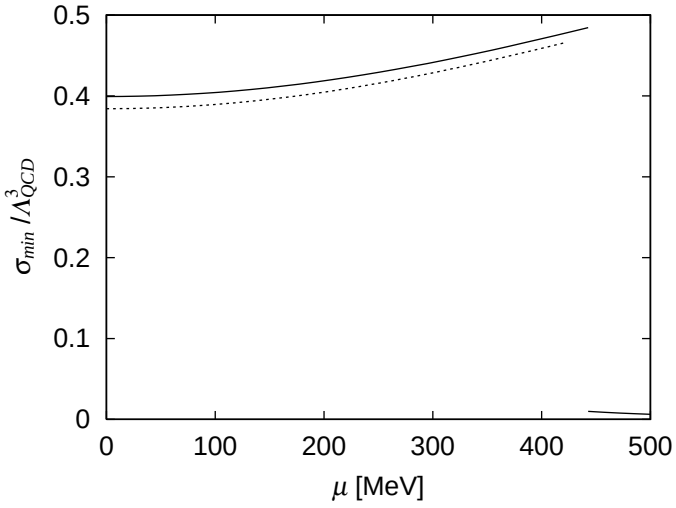

FIG. 12. The chemical potential dependence of σ_{min} at $T = 0$. The curves show the cases $m_R(1\text{GeV}) = 7$ MeV (solid line) and the chiral limit (dotted line).

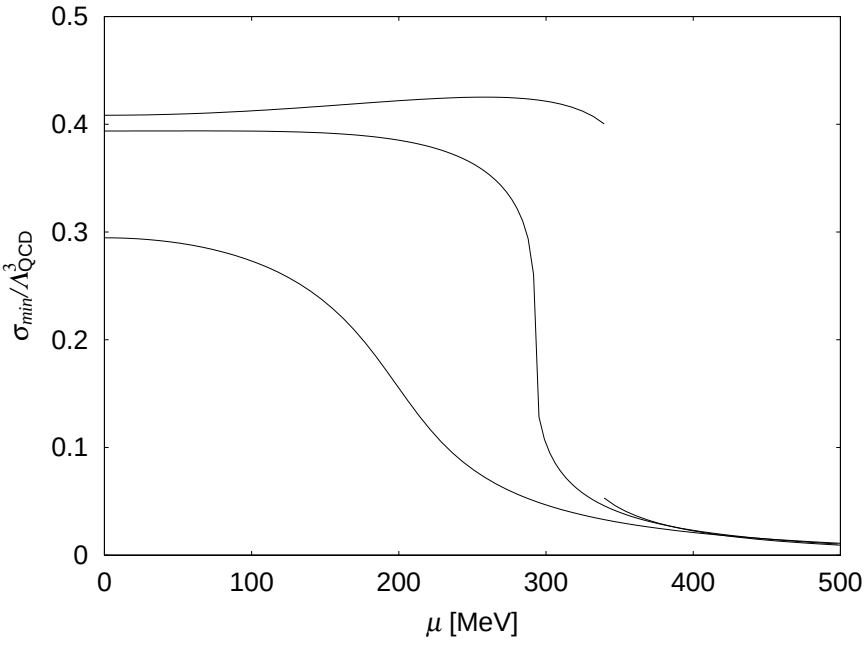

FIG. 13. The order parameter σ_{min} as a function of μ for (top to bottom) $T = 80, 95, 120$ MeV.